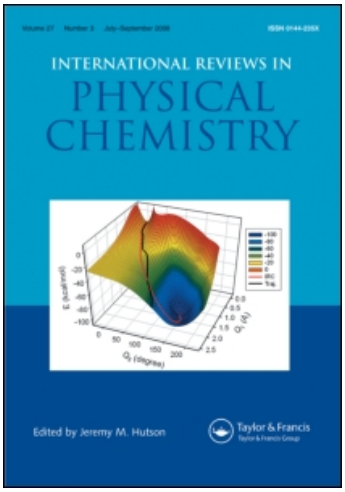

International Reviews in Physical Chemistry
Publication details, including instructions for authors and subscription information:
http://www.informaworld.com/smpp/title~content=t713724383

Oriented xenon hydride molecules in the gas phase

Udo Buck[a]; Michal FáRníK[b]
[a] Max-Planck Institut für Dynamik und Selbstorganisation, Bunsenstr, 10 D-37073 Göttingen, Germany
[b] J. Heyrovský Institute of Physical Chemistry, Academy of Sciences of the Czech Republic, Prague 8, Czech Republic

Online publication date: 11 October 2010

To cite this Article Buck, Udo and FáRníK, Michal(2006) 'Oriented xenon hydride molecules in the gas phase', International Reviews in Physical Chemistry, 25: 4, 583 — 612
To link to this Article: DOI: 10.1080/01442350600847746
URL: http://dx.doi.org/10.1080/01442350600847746

International Reviews in Physical Chemistry,
Vol. 25, No. 4, October–December 2006, 583–612

Taylor & Francis
Taylor & Francis Group

Oriented xenon hydride molecules in the gas phase

UDO BUCK*† and MICHAL FÁRNÍK‡

†Max-Planck Institut für Dynamik und Selbstorganisation,
Bunsenstr. 10 D-37073 Göttingen, Germany
‡J. Heyrovský Institute of Physical Chemistry, Academy of Sciences
of the Czech Republic, Prague 8, Czech Republic

(*Received 11 May 2006; in final form 7 June 2006*)

The production of the xenon hydride molecules HXeX with X = I and Cl in the gas phase is reviewed. These molecules are generated by the photolysis of the hydrogen halide HI and HCl molecules on the surface of large xenon Xe_n clusters. Molecular dynamics simulations show that the flexible H atoms react with the heavy XeX moiety and form the desired molecules with nearly no rotational motion. They are observed by photodissociation with subsequent detection of the kinetic energy of the H atom fragment. During the generating process, the cluster starts to evaporate and the hydride molecule is left essentially free. For further discrimination against the H atom fragments from HX, the HXeX molecules are oriented in a combined pulsed laser field and a weak electrostatic field. The three topics which represent the background of our experiments are briefly reviewed: the nature and generation of rare gas hydrides, the alignment and orientation of molecules in electric fields, and the photodissociation of selected molecules in rare gas clusters. The conditions for detecting them in the gas phase are discussed. This is the trade off between the stability, which requires high electron affinity, and the conditions for orientation, which necessitate large polarizability anisotropies and dipole moments. Finally the prospects of detecting other classes of molecules are discussed.

Contents

*Corresponding author. E-mail: ubuck@gwdg.de

International Reviews in Physical Chemistry
ISSN 0144–235X print/ISSN 1366–591X online © 2006 Taylor & Francis
http://www.tandf.co.uk/journals
DOI: 10.1080/01442350600847746

1. Introduction

A couple of years ago, we started a series of experiments on the photodissociation of hydrogen halide molecules which were located in different environments of rare gas clusters [1]. The idea behind these experiments was to elucidate the molecular mechanisms of the influence of the solvent on the important process of the unimolecular fragmentation in the condensed phase. Clusters have the advantage that the number of constituents is finite, that the properties can be investigated as a function of the size, and, last but not least, that special experimental observables are accessible which are otherwise difficult to get. A typical example is the measurement of the kinetic energy of one of the fragments. The result is a direct reflection of the dynamical interaction of the molecule with the solvent. In the case that the fragment leaves the cluster with a high kinetic energy, close to that of the free molecule, there is nearly no interaction with the surrounding cage atoms and we talk about the direct cage exit. If, in contrast, the kinetic energy is close to zero, the interaction with the solvent atoms is so strong that the fragment remains in the cage.

The experiments were operated for the three hydrogen halides HCl, HBr, and HI, and the four host clusters of neon, argon, krypton, and xenon. We measured the kinetic energy distribution of the outgoing H atoms. We got several quite interesting results on the exit probabilities of the investigated hydrogen halides depending on the exact surface position and the number of surrounding shells for the interior positions [2–5]. We also observed an unexpected dependence on the host clusters. For neon clusters, we measured and analysed that the outer shell turned out to be liquid [6]. But this is not the topic of this review. For the dissociation of HI molecules in Xe_n clusters, we observed that the time-of-flight spectra were rather asymmetric [7, 8]. As outlined below, the only reason for such a behaviour could be that we dissociated an oriented molecule. The clarification of this effect will be the subject of this article. It turned out to be relatively easy to find the right molecule for such a process. It should contain a hydrogen atom, a xenon atom and an iodine atom. Thus HXeI would be the

easiest solution. Such molecules were observed, indeed, in matrices. They belong to a new class of rare gas hydride compounds which are mainly bound ionically and which are produced by the photolysis of HI molecules in xenon matrices. The production process in matrices and large clusters should have some similarities. It was much more difficult to understand the orientation of this molecule in our experimental arrangement. It was again relatively easy to realize how such a molecule was aligned in our apparatus, which means that the molecule is stabilized in the direction of an applied electric field, independent of the two different ends. Our large oscillating laser field interacts with the anisotropy of the polarizability of the molecule. The latter one is in fact quite high for a molecule which contains Xe and I atoms and explains the effect. But this does not account for the orientation of the molecule which selects one direction only. The standard procedure requires the interaction of a dipole moment with an electric field which is usually three orders of magnitude larger than what we had in our experiment. Here the recent proposal of Friedrich and Herschbach pointed the way out of the problem [9, 10]. They suggested that the coupling of a strong laser field with a weak static electric field changes the alignment of the molecule into an orientation provided that the molecule exhibits the appropriate polarizability and dipole moment. A further complication arises by the fact that the molecule has to be kept away from the energetically closely lying state with the opposite orientation. Here the profound spectroscopic knowledge and the clear way of thinking of the late Roger Miller came into play. After a contribution by one of us at an international conference, he pointed out these problems and gave us also the advice to look for an experimental proof that this procedure was operating in our experiments. We solved both problems and would like to give him the credit for his clear judgment and his deep understanding of the underlying physics.

In this project we have to deal with the rather interesting overlap of three completely different research fields. These are the generation of a new class of rare gas containing molecules, the photodissociation of molecules in clusters, and the orientation of molecules in electric fields. Since the people who are equally familiar with all three fields are probably not too numerous, we found it quite interesting to present our results in a larger context. We used the photolysis of HX molecules in Xe_n clusters to prepare the desired molecules HXeX. We detect these molecules by the photodissociation and subsequent detection of the H atoms. To discriminate against the photoproducts of HX, the HXeX molecules are oriented in a combined strong laser field and a weak electrostatic field. In fact, our experiments were the first ones in which such molecules were detected in the gas phase and one of the first experimental verifications of the proposed method of Friedrich and Herschbach for obtaining oriented molecules.

We will start this review with a detailed description of the foundations and the three methods applied in this experiment. Then we will present the experimental setup and treat the results of the two prototype molecules HXeI and HXeCl. We will continue with a discussion of the failure and the success of detecting other molecules and close with a comparison of this method with other procedures and a discussion of future perspectives.

2. Background information

2.1. *Rare gas hydride compounds*

In 1995 the group of Räsänen discovered a new class of rare gas containing molecules [11]. They have the general structure HRgX, where Rg is a rare gas atom, usually Xe, Kr, and in exceptional cases also Ar, and X is an electronegative atom or radical. The experiments were carried out in low-temperature rare gas matrices and usually initiated by the photodissociation of a precursor molecule which contains both the H and the X component. At the end of 2004 twenty compounds of this type were detected. Most of them are linear, with Xe as rare gas atom and halogen atoms for the electronegative element [12]. For further authoritative reviews on this topic we refer to [13–15].

The HRgX compounds are quite stable molecules with a strong ionic character. The nature of the bonding can be best described as HRg^+X^- which underlines the mostly ionic bonding between Rg and X and the mostly covalent bonding between H and Rg. After the photodissociation of HX and the excitation to a manifold of neutral interaction potential surfaces, also the charge transfer states become accessible. This is pictorially shown in figure 1 for the system HXeI. The avoided potential crossing leads to a decay of the ionic system over a small barrier into neutral fragments. Extensive electronic structure calculations confirm this simplified picture and indicate a substantial charge transfer character [16–19]. It is noted that there is still a smaller covalent component present in these bonds. The strength of the bonding depends on the electron affinity of the X component and on the size of X^-, since smaller fragments allow a closer approach and thus a stronger stabilization by the Coulomb interaction. At the positive end, the ionization potential of the Rg atom and the bonding of HRg play a role. Thus the dissociation energy of HXeI is 0.42 eV with distances of 1.74 Å

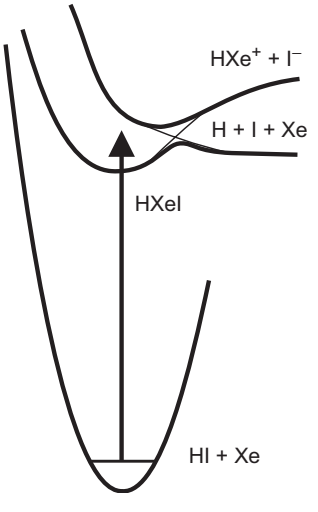

Figure 1. Schematic view of the potential surfaces that determine the bonding properties of HXeI.

for H–Xe and 3.10 Å for Xe–I [13, 20], while that of HXeCl amounts to 0.9 eV with 1.69 and 2.66 Å for the H–Xe and Xe–Cl distances, respectively [13, 17]. A deeper well of 1.43 eV has been found for HXeCN [21]. This behaviour mainly reflects the increasing electron affinity of the X component.

We note that these values correspond to metastable local minimum structures which decay into the neutral H + Xe + X fragments when the molecule is stretched. The other dissociation channel which follows the bending motion of the HRgX molecule into the van der Waals complex Rg + HX, is very exoergic but usually hindered by a barrier which is larger than the dissociation energy into the other channel. While the latter one is relatively easy to calculate using second-order Møller-Plesset (MP2) perturbation theory, this is quite difficult for the reaction path into three neutral particles. Here multi-reference configuration interaction (MRCI) methods have to be used. We present in figure 2 the results for HKrF obtained by Gerber and coworkers [22], one of the few examples where both barriers were calculated. As already mentioned earlier, the barrier to H + Kr + F following the stretching coordinates is with 0.26 eV much smaller than those of the bending motion which amounts to 1.4 eV. The energy release exhibits a similar behaviour with 0.94 and 4.9 eV, respectively. The calculated value of the barrier for the bending motion of HXeCl is 1.4 eV and the energy released after this barrier is overcome amounts to 4.0 eV [17]. For HXeI the energetics have been obtained experimentally using the infrared induced pumping and decomposition [20]. The minimum energy for the dissociation into H + Xe + I is 0.42 eV with a barrier of 0.087 eV.

These molecules are mainly prepared in two ways which reflect the inversion of the decay channels. In the first step atomic hydrogen H and the X fragments are generated by photodissociation of the HX molecule in the low-temperature solid Rg matrices at 30 K. Then the temperature is raised up to the point at which the H atoms start to migrate and the HRgX molecules are formed by the recombination reaction

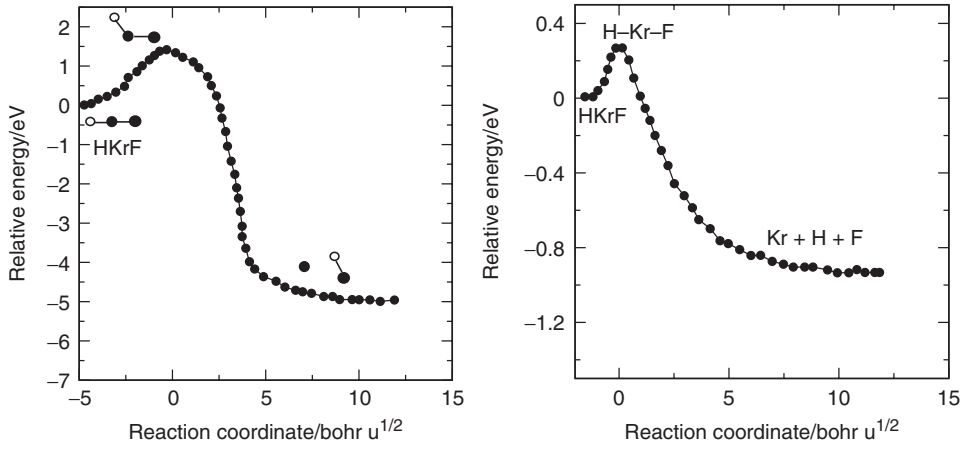

Figure 2. Minimum energy paths for the reactions HKrF → Kr + HF (left) and HKrF → H + Kr + F (right) [22]. The mass weighted coordinates are the bending and the stretching motion, respectively.

$H + Rg + X \rightarrow HRgX$. The yield is high and the mechanism requires long-range migration or even diffusion before the final product is formed. In a small number of cases, a different mechanism was found. In the case of the photolysis of HCl in Kr matrices, the intermediate HKrCl was found after only a short range travel from primary dissociation [23, 24]. In this case the HRgX molecule is formed directly by the photodissociation of HX, the motion of the H atom to the next Rg layer, and the recoil to a transition state of the configuration H–Rg–X. Such a process has been simulated by molecular dynamics in which the non-adiabatic transitions were included [25]. The time scale is indeed very fast, on the order of a few picoseconds. The experimental yield in this case is smaller than in the first case, since the molecule HRgX is destroyed by the secondary photolysis by the same radiation used for the dissociation of HX, via the process $HRgX + h\nu \rightarrow H + Rg + X$. It is obvious that the first, long range mechanism will not operate for clusters in the gas phase. The fast, short range one is much more appropriate. As will be demonstrated later, we will use the photodissociation directly for the detection of the HRgX molecule.

In matrices, the HRgX molecules are detected by the infrared spectroscopy of the very strong H–Rg stretching absorptions. They provide essentially most of the experimental observation on the bonding properties and the decay mechanisms which were discussed in this section. Further interesting issues in the experiments in solid matrices are the extension of the hydride molecules to other electronegative species X than those of HXeCN already mentioned. These include HXeNCO [26], HXeOH [27], HKrCCH [28], and HXeCCH [24] which opens the gate to a novel organo-rare gas chemistry. In addition, also complexes of the new hydride molecules with N_2 [29] and H_2O [30] have been investigated.

2.2. *Orientation of molecules*

The orientation and alignment of molecules are very well established quantities to be measured in molecular beam experiments. They indicate the direction of the angular momentum vector **J** with respect to the given direction of the molecular axis **R** which, in turn, is defined by an electric field **E**. The **J** vector is oriented if the angular momentum is parallel or antiparallel to the field. The distribution of **J** is aligned if the **J** vectors are parallel and antiparallel or perpendicular to the field. The standard method to achieve orientation is the interaction of symmetric top molecules in hexapole electric fields by the first-order Stark effect [31]. The interaction of the permanent dipole moment μ with the static electric field E_s is given by

$$V = -\mu E_s \cos\theta, \tag{1}$$

in which θ is the angle between the molecular axis and the electric field E_s. For large values of this energy in terms of the rotational constant

$$\omega = \mu E_s / B \tag{2}$$

the more versatile method of pendular orientation results. Here the rotor states are converted into pendular librators confined to oscillate about the field direction. The pendular states are hybrids comprised of linear combinations of field free rotor states J, M with the same M but different J values [32]. The procedure has been applied to symmetric top and linear molecules [33–35]. The by far largest value of $\omega = 360$ was obtained by Roger Miller in the experiments with the linear trimer of hydrogen cyanide [36]. In practical units, the interaction parameter ω is given by $\omega = 0.0168\mu(\text{Debye})\ E_s(\text{kV cm}^{-1})/B(\text{cm}^{-1})$. This relation shows that this method is restricted to molecules with large dipole moments and rather high strength of the electric field.

To extend such a procedure to a much larger class of molecules, Friedrich and Herschbach proposed to use instead of the permanent dipole moment, the polarizability α which leads to an induced dipole moment. Generally, such induced moments are weak, but with the intense non-resonant laser fields which are now available, the method appears to be feasible. The interaction is given by

$$V = (2\pi I_l/c)\left[(\alpha_\parallel - \alpha_\perp)\cos^2\theta + \alpha_\perp\right], \tag{3}$$

with the laser intensity I_l and the polarizabilities $\alpha_\parallel$ parallel and $\alpha_\perp$ perpendicular to the molecular axis. The laser intensity is related to the electric field vector E_l by $I_l = (c/4\pi)E_l^2$. It is convenient to introduce the dimensionless interaction parameter

$$\Delta\omega = 2\pi I(\alpha_\parallel - \alpha_\perp)/(Bc). \tag{4}$$

In practical units we get $\Delta\omega = 10^{-11}\Delta\alpha\ (\text{Å}^3)\ I_l\,(\text{W cm}^{-2})\ /\ B\ (\text{cm}^{-1})$. It is obvious from the interaction that in this case the molecules are aligned along the axis of the laser field and still contain parallel and antiparallel directions. Experiments were carried out for a series of diatomic and polyatomic molecules [37] which showed this effect. An interesting extension of this work was employed by Stapelfedt and coworkers [38]. By replacing the linearly polarized light with elliptically polarized light they forced an asymmetric top molecule to align along all three axes in space.

If the non-resonant radiation is delivered as a pulse of intensity $I(t) = I_0 g(t/\tau)$, with I_0 the peak intensity, $g(t/\tau)$ the pulse time profile, and τ the pulse duration, the anisotropy parameter $\Delta\omega = \Delta\omega(t)$ and the induced dipole potential become a function of time. The corresponding time-dependent Schrödinger equation, with a time dependence determined by the time profile $g(t/\tau)$ of the pulse, can be cast in a dimensionless form by dividing through B. As a result, the equation clocks the time in units of $\hbar/B$ which defines a 'short' and a 'long' time for any molecule and pulse duration. The analysis [39] of the time dependence shows that in the long-pulse limit ($\tau \approx 5\hbar/B$), the interaction is adiabatic and the pendular states faithfully follow the field as if it were static at any instant.

The last step in the development of oriented molecules is a combined application of the static electric field and a non-resonant laser field proposed by Friedrich and Herschbach [9, 10]. If the fields are parallel, the angular amplitude of the pendular states is narrowed by the enhanced hybridization of the J states. For certain pairs

of states, which become nearly degenerate tunnelling doublets in the laser field, even a weak static field can induce a strong orientation with the help of a pseudo-first-order Stark effect. The effect occurs for any polar molecule, since in addition to the dipole moment only an anisotropic polarizability is required.

The orientation of the molecular axis in a given state is characterized by its orientation cosine, $\langle\cos\theta_s\rangle$, in which θ_s is the polar angle between the molecular axis and the direction of the electrostatic field E_s. Note that $\theta_s^0 = \arccos\langle\cos\theta_s\rangle$ are the angular amplitudes of the molecular axis in the field; the greater the orientation cosine the smaller the angular amplitude. Figure 3 shows the dependence of the $\langle\cos\theta_s\rangle$ for the members of the lowest tunnelling doublet, the $\tilde{J}=0, M=0$ and $\tilde{J}=1, M=0$ states, as functions of $\Delta\omega$ at fixed (small) values of ω for congruent (parallel or antiparallel) fields. The two states are oriented opposite with respect to one another, with the consequence that their mixture would exhibit alignment only. One can also see that at high enough $\Delta\omega$, the orientation always becomes nearly 'perfect', with an angular amplitude of less than $\pm 20^\circ$ for either state. Since the angular amplitude of the alignment θ_l^0 is always smaller than θ_s^0, the strong orientation effect can also be regarded as arising from the restriction on the angular amplitude of the molecule imposed by the intense radiative field: once the radiative field couples the molecular axis to its field vector E_l, the permanent dipole, which lies along the same molecular axis, has no choice but to remain within the range preordained by the radiative field; the parallel static field just serves to define a preferred direction. Note that for $\omega \ll \Delta\omega \geq 10$ and the $\tilde{J}=0, M=0$ or $\tilde{J}=1, M=0$ doublet, the values ω_p and $\Delta\omega_p$ of the interaction parameters which yield a 'perfect orientation' are approximately related by $\omega_p \approx 2 \times \exp(-0.11 \times \Delta\omega_p)$. So for instance, if $\Delta\omega_p = 100$ can be attained (which is the case for most molecules, even in a laser pulse long enough to warrant adiabaticity), $\omega_p = 10^{-5}$ would correspond, for a molecule with $\mu/B = 1$ Debye/cm^{-1}, to a truly small electrostatic field of just 0.5 mV/cm. The first experimental application of this method was our experiment on the HXeI molecules which is described in detail in this review [7, 8].

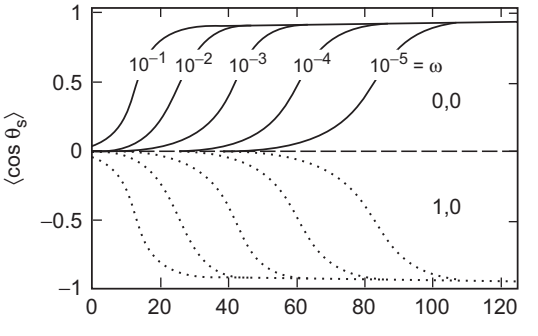

Figure 3. The dependence of the orientation cosine $\langle\cos\theta_s\rangle$ for the members of the lowest tunnelling doublet, the $\tilde{J}=0, M=0$ and $\tilde{J}=1, M=0$ states, as functions of $\Delta\omega$ at fixed values of ω for congruent fields. The two states are oriented opposite with respect to one another.

2.3. *Photodissociation of molecules in clusters*

The idea of our experiments on the photodissociation of molecules which are placed in the interior or on the surface of large clusters was already presented in the introduction. We will give here only a short account of the detection system, since this plays a crucial role in the interpretation of the data which are obtained for oriented molecules.

The field of photodissociation of bare molecules is very well developed with a number of sophisticated detection techniques ranging from Doppler and time-of-flight spectroscopy [40, 41] over laser induced fluorescence [41] to the photofragment imaging techniques [42, 43]. We are in particular interested in the detection of H atoms. For these atoms Welge and coworkers [44] have invented the elegant technique of Rydberg tagging. Instead of ionizing the nascent neutral H atom by a resonance enhanced multi-photon (REMPI) process, the H atoms are excited to a high Rydberg state and fly as neutrals to the detector where they are ionized by a small electric field. Since we are interested in detecting H atoms with small or even zero velocity, we have to apply more conventional techniques where the translational distribution of the neutral photofragments are monitored by the ion. By applying a small electric field we extract those ions already flying in the direction of the detector and turn around those ones that start in the opposite direction. From the different arrival times the velocity is calculated [45].

Our experimental arrangement for the detection is schematically shown in figure 4. The hydrogen halide molecules HX in or on the cluster beam are dissociated by a focused pulsed laser beam. By changing the polarization of the laser, the angular dependence of the photodissociation is measured. This is pictorially demonstrated in figure 4. For 90° polarization of the laser only the fragments of those molecules with perpendicular transition moment with respect to the molecular axis can reach the detector (middle part). For 0° polarization, essentially molecules with a parallel transition moment are detected (right-hand part).

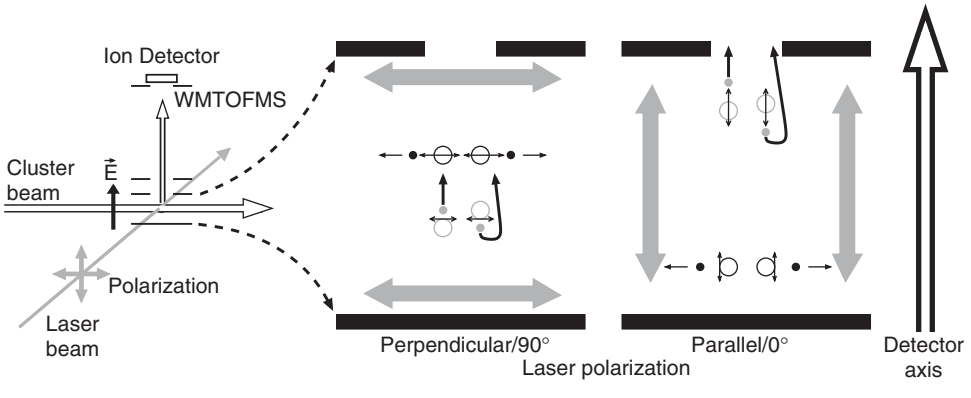

Figure 4. Schematic view of the detection arrangement in the left part. The middle and right parts explain the geometric conditions in the time-of-flight mass spectrometer (TOFMS). The laser beam propagates perpendicularly to the plane of the paper. White circles depict the X atoms, small grey or black circles represent hydrogen atoms, and tiny double-headed arrows indicate the transition dipole moment of the HX molecules.

What is actually measured in the experiment is the kinetic energy of product H atoms by analysing the trajectories of the ions. The different contributions which can be derived from the measured kinetic energy of the H atom $E_{kin}(H)$ are best discussed by the energy balance of the process

$$h\nu + E_{int}(HX) = D_0 + E_{int}(X) + E_{kin}(X) + E_{kin}(H) + E_{clu}, \quad (5)$$

where the excitation wavelength $h\nu$ and the dissociation energy D_0 of HX are known, and $E_{kin}(H)$ is measured. By conservation of momentum, the kinetic energy of the X atoms $E_{kin}(X)$ is also known. The excitation of the spin–orbit state X^* in the halide X product channel is presented by $E_{int}(X)$ and is measured as energy loss in the kinetic energy of the H atom $E_{kin}(H)$. These effects would also appear in the dissociation of HX monomers and indicate the direct cage exit. The influence of the cluster is expressed by the continuous energy loss E_{clu} of the H atoms caused by the collisions with the cage. This leads, depending on the position and the interaction, to delayed cage exits or complete caging if the velocity is zero. The internal excitation of the HX molecule before the dissociation $E_{int}(HX)$ is observed as energy gain. In general, the molecules will be in the ground state after the expansion so that in the experiments presented here, this effect does not occur.

The way how to extract from this information the kinetic energy distribution is described in detail in [46] and [47]. The key is a complete simulation of the ongoing process. First, the angular distribution of the photodissociation, the laser polarization, and the kinetic energy E_{kin} are the input parameters. Then the velocity distribution of the molecular beam, the finite interaction volume, the detector dimensions, and the acceleration of the ion trajectories are all accounted for and lead to the calculation of time-of-flight spectra for the input kinetic energy. These resulting simulated spectra are then fitted to the measured spectra using a least-square fitting algorithm and the corresponding best fit centre-of-mass distributions for the kinetic energy are obtained. We note that in our experimental arrangement, the detection probability is extremely enhanced at small kinetic energies so that we are in particular sensitive to the caged atoms [46]. The reason is the lower transverse velocity and the larger solid angle compared to faster fragments.

Figure 5 shows a representative H fragment time-of-flight (TOF) spectrum from the photodissociation of pure HI molecules generated by the coexpansion of 8% HI seeded in Ar at room temperature. The outer peaks originate from the photodissociation of HI with the iodine partner fragment in its spin–orbit ground state. The inner peaks correspond to H fragments with a partner fragment I^*. These H atoms appear later in the forward part because of their lower kinetic energy corresponding to the higher internal energy of the iodine atom. If their trajectories point initially away from the detector their lower kinetic energy causes them to be slowed down more easily, which results in an earlier appearance in the rear part of the spectrum (see also figure 4). In figure 5 the measurement is represented by circles. The solid line corresponds to a fit carried out by our Monte Carlo particle trajectory simulation program [47]. For this fit we use values for the anisotropy parameter of the angular distribution β and the branching ratio R from the recent publication

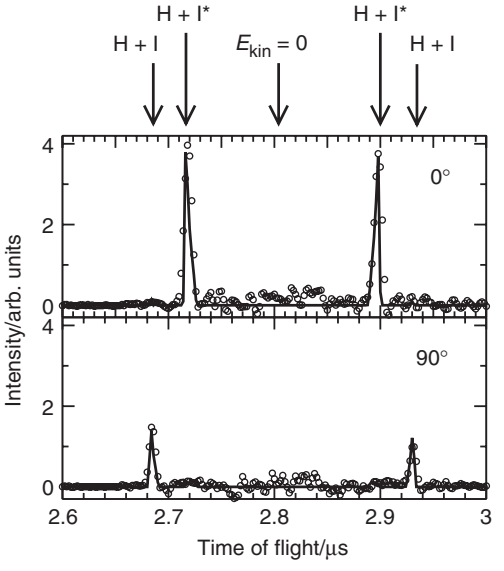

Figure 5. H atom TOF spectra from the photodissociation of pure HI molecules. The measurement is represented by circles. The solid lines correspond to the TOF spectra from the Monte Carlo trajectory simulation program which also accounts for the theoretical prediction of the dissociation process [48].

of Le Roy and coworkers [48] ($\beta(I) = -1.00$, $\beta(I^*) = 2.00$, $R = 0.934$). The excellent agreement between fit and measurement proves the reliability of our data and the data evaluation procedure. The outer peaks have less intensity because of a lower detection efficiency for higher energy particles due to their higher transverse velocity [46]. We note that none of the molecules with the 'wrong' orientation reaches the detector.

When the dissociation process takes place in a cluster environment the H fragment trajectories are influenced by the cluster cage. A typical result for HI molecules prepared by pick-up on Ne_n clusters with $n = 143$ at a laser polarization of 90° is shown in figure 6. We observe the two outer peaks which correspond to direct cage exit events and a large peak in the middle which originated from H atom with zero velocity. There is, as expected small, unstructured intensity in between. Our measured time-of-flight spectra can be transformed into H atom kinetic energy distributions using a least-square fit method with the above mentioned program. The result is displayed in the lower part of figure 6. We would expect the peak for the direct cage exit at 2.05 eV based on the dissociation energy D_0 of HI (3.055 eV) [49]. The peak is indeed at the correct position. For the excited spin–orbit state the predicted energy is 1.11 eV. The somewhat washed out peak at this position is already an indication that it results mainly from scattered and slowed H atoms. The dominating peak is that of H atoms with zero velocity. We note that the process of slowing the H atoms transfers an appreciable amount of energy to the cage so that the cluster starts to evaporate [50]. This makes the detection of H atoms with small velocities much easier so that most of them can be extracted after the ionization by the electric field and reach the detector.

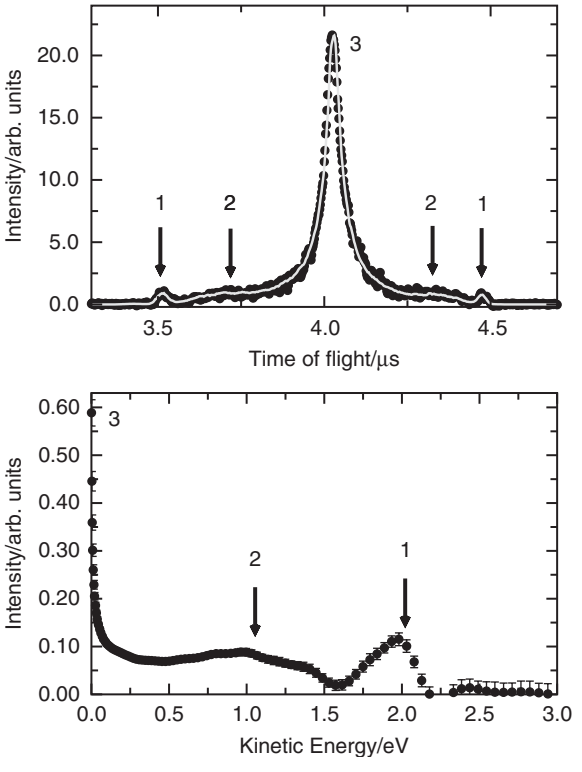

Figure 6. Time-of-flight spectra and kinetic energy distribution of the H atoms from the photodissociation of HI–Ne_n for the laser polarization of 90°. (1) direct cage exit to the ground state, (2) delayed cage exit, (3) complete caging.

3. Experimental

The oriented xenon hydride molecules were prepared in the experimental apparatus for photodissociation studies of molecules in various cluster environments [1], described in more detail elsewhere [1, 47, 51]. The experiment is shown schematically in figure 7. Briefly, the xenon cluster beam was produced by a supersonic expansion of neat Xe gas through a nozzle of conical shape with 60 μm diameter, 30° opening angle, and a length of 2 mm. The expansion pressures and nozzle temperatures which determined the mean cluster sizes are summarized in table 1. After passing through a skimmer followed by a differentially pumped vacuum chamber, the cluster beam entered a pick up cell filled with the molecular gas. The gas pressure of 4×10^{-2} mbar was chosen such that mainly single molecules were attached to the clusters. Recent molecular dynamics simulations of similar systems showed that the hydrogen halide molecules attached in the pick-up process will stay in a substitutional position in the surface layer [3, 6].

The clusters with the attached molecules then entered a detection chamber with two-stage time-of-flight spectrometer of the Wiley–McLaren type (WMTOF).

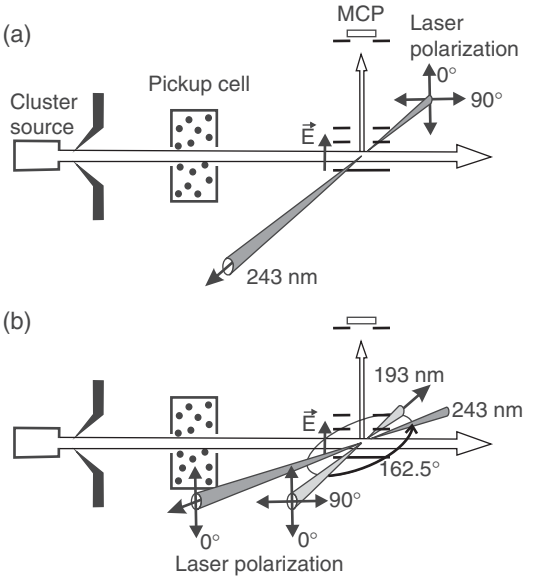

Figure 7. Schematic view of the experimental apparatus. (a) 243 nm laser beam only, and (b) 193 nm dissociation and 243 nm ionization laser beams.

Table 1. Experimental conditions.

Expansion gas		Xe	
Picked-up molecule	HI: exp1	HI: exp2	HCl
Expansion pressure (bar)	1.0–3.5	3.0–5.0	5.0
Nozzle temperature (K)	220–279	203–218	243
Average cluster size $\langle n \rangle$	110–830	107–2017	1020
Laser intensity (10^{11}W cm^{-2})			
243 nm	1.2	0.55	0.44
193 nm	–	–	1.14
WMTOF extraction field (V cm^{-1})	4.2	4.2	7.8

It is surrounded by a copper shield kept at a temperature of 20 K by a high-pressure compressor to suppress the unwanted H atoms from the photodissociation of the background gas, i.e. mainly pump fluid hydrocarbons. The background vacuum in the chamber was maintained at approximately 10^{-9} mbar with the beam operating. Here the molecules on clusters were photolysed by the laser light, then the H fragments were ionized, and the spectrometer was used to analyse the velocity distributions of the H atoms arising from the photodissociation process. For this purpose the WMTOF was operated in the so called low-field mode with a small electric field applied to extract the ions to the detector. As already outlined above, with this extraction field, ions could be detected with initially zero velocity or even with the velocity vector pointing in the opposite direction with respect to the direction towards the detector, and their velocities could be analysed. Since the extraction field intensities, were essential for

the HRgX molecule orientation, as discussed earlier, the voltages were also summarized in table 1.

Laser radiation with the wavelength of 243 nm was used for photoionization of H atoms via the one-colour, resonance enhanced multi-photon ionization (REMPI) in a (2 + 1) excitation scheme. At the same wavelength the HI molecules attached to the rare gas clusters were photolysed, and also the generated HXeX molecules were dissociated at this wavelength. For photolysis of the HCl molecules the wavelength of 193 nm was used. However, for the H fragment detection the same REMPI process at 243 nm was employed.

The wavelength of 243.06 nm was generated by mixing the fundamental of a Nd:YAG laser (Quanta Ray GCR-5) with the frequency doubled output of a dye laser (LAS, LDL 20505) operated at 630.3 nm, and pumped by the second harmonic of the Nd:YAG laser. The laser pulses were repeated at a frequency of 10 Hz with a pulse duration of 5 ns. The laser beam was focused into the detector chamber by a 400 mm quartz lens onto a spot of 14 μm radius (Gaussian beam waste), in the intersection point of the cluster beam and the WMTOF axis. The laser beam, the cluster beam, and the WMTOF axis were mutually perpendicular to each other (see figure 7a) to eliminate the Doppler effects in the photodissociation measurements. A typical UV laser output energy was 4 mJ/pulse. The effective laser intensities at the focal spot interacting with the molecular beam were again summarized in table 1. The polarization of the linearly polarized laser light could be turned parallel (0° polarization angle) or perpendicular (90° polarization angle) with respect to the WMTOF axis by passing the beam through a series of prisms.

In the experiment with the HCl molecules additionally an ArF/F_2-excimer laser (Lambda: Compex 102) was implemented for the molecule dissociation at 193 nm. The emitted light was polarized using a thin film polarizer (TFP), and sent into the detector chamber perpendicularly to both, the cluster beam and the WMTOF axis (see figure 7b). The rotation of TFP about the laser beam axis allowed to change the laser light polarization from 0° to 90° polarization angle with respect to the WMTOF axis. The laser beam is focused by a 366 mm LiF lens onto a spot of radius approximately 10 μm. A typical laser energy was 12 mJ over 20 ns pulse length. This translated to the effective laser intensity of 1.1×10^{11} W cm^{-2} in the focal spot interacting with the molecular beam, similar to the above 243 nm laser intensities (see table 1). After the dissociation the H fragment ionization proceeded as above with the 243 nm laser beam. In this experimental arrangement the ionization laser beam was introduced into the detector chamber at 162.5° to the dissociation beam, in the plane of the cluster beam and the dissociation laser beam (see figure 7b). The polarization of the ionization laser light was parallel to the WMTOF axis (0° polarization).

The time synchronization of the two laser beams was achieved by triggering the excimer laser by the Nd:YAG laser pulses via a pulse delay generator. Experimentally challenging was the spatial overlap of the two laser beams focused to approximately ~10 μm with the intersection point of the cluster beam and the WMTOF axis. The tight laser light focusing into a small spot in the interaction region was important, since the molecule alignment and orientation depend strongly on the electric field intensity of the laser light combined with the extraction electric

field of the WMTOF, as outlined below. The overlap was adjusted with the intensity and symmetric shape of a test HBr/Ar_n system.

4. Formation and orientation of the molecules

The mechanism of the HXeX generation has been briefly outlined above. It is obvious that the delayed mechanism with an appreciable migration of the H atom like in solid matrices does not take place in clusters with their finite dimensions. In fact, the process has been simulated using Molecular Dynamics for HXeCl following the photolysis of HCl in Xe_n clusters by Gerber and coworkers [25]. Based on simplified but reliable potential models for all excited states of neutral and ionic character and the non-adiabatic couplings between them, the following dynamics resulted. They are pictorially shown in figure 8. The photoproduced H atoms leave the reagent cage, hit the second wall of Xe atoms, and are recoiled towards the Xe atom of the cage. Then rapid charge transfer takes place and the HXeCl molecules with their ionic bonding properties are formed. It turned out that the ionic character of the new molecule plays an important role in the stabilization of the molecule by the strong coupling to the cluster vibrations which removes additional energy from the nascent HXeCl.

After the strongly polarizable HXeX molecule is created, it is forced to align in the direction of the plane-polarized electric field of the laser beam, by the interaction of the polarizability anisotropy with the laser field, as outlined in Section 2.2. This still allows the molecule to point in two opposite directions in the polarization plane. The additional weak extraction electric field of the WMTOF can orient the linear molecule, interacting with its permanent dipole moment by the so-called pseudo-first-order Stark effect. At the 0° laser beam polarization the orientation is such that the H atom points towards the detector. To check if the conditions of orientation as outlined in figure 3, we present the data of several HXeX molecules together with those for HI in table 2. The values of $\Delta\alpha$ were calculated from the polarizability α of the constituents using a relation between $\Delta\alpha$ and α derived from similar ionically bound systems. It is obvious that HI cannot be oriented in our apparatus. Let us take HXeI as example. The value of $\Delta\omega = 70$ is large enough to align the $\tilde{J} = 0, M = 0$ and $\tilde{J} = 1, M = 0$ states of the HXeI molecule with an angular

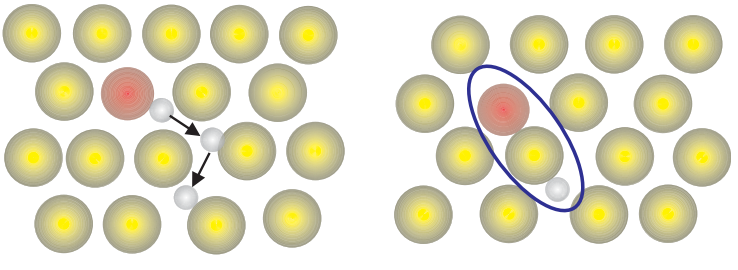

Figure 8. Formation of HXeCl after the photodissociation of HCl in Xe clusters [25]. Xe: gold (bright), Cl: red (dark), H: white.

Table 2 Characteristic data for the orientation of different molecules: $\Delta\alpha$ anisotropy of dipole polarizabilities (geometries from [13]), B rotational constant, μ dipole moment [13], $\langle\cos\theta_s\rangle$ orientation cosine. The dimensionless parameters ω and $\Delta\omega$ are are defined in equations (2) and (4). Polarizabilities for HI are from [62].

Molecule	$\Delta\alpha$/Å^3	B/cm^{-1}	μ/D	ω	$\Delta\omega$	$\langle\cos\theta_s\rangle$	θ_s/deg
HI	0.43	6.551	0.45	0.005	0.072	0.002	90.0
HXeI	3.4	0.0268	6.41	0.016	70	0.936	20.6
HXeBr	2.5	0.0420	7.33	0.012	26	0.583	54.3
HXeCl	2.2	0.0843	7.25	0.011	41	0.910	24.5
HKrCl	1.6	0.0960	9.35	0.012	26	0.583	54.3

amplitude of just $\pm 20^\circ$. Our electric field $E_s = 4.2$ V/cm gives rise to $\omega = 0.016$; however, even $\omega \approx 10^{-3}$ would be enough to strongly couple the $\tilde{J} = 0, M = 0$ and $\tilde{J} = 1, M = 0$ states and thus 'perfectly' orient them (for $\Delta\omega_p \approx 70$, $\omega_p \approx 10^{-3}$). The orientation cosines of the two states at $\omega = 0.016$ and $\Delta\omega = 70$ are $\langle\cos\theta_s\rangle_{0,0} = 0.936$ (along the static field) and $\langle\cos\theta_s\rangle_{1,0} = -0.936$ (opposite to the static field). While the $\tilde{J} = 0, M = 0$ state correlates with the rotational ground state (whose $J = 0$) of the HXeI molecule, the $\tilde{J} = 1, M = 0$ correlates with the first excited rotational state (whose $J = 1$). Since the energy difference between the $\tilde{J} = 0, M = 0$ and $\tilde{J} = 1, M = 0$ states is quite small, about 0.03 B at $\Delta\omega = 70$ and $\omega = 0.016$, a separation between them cannot be attained by cooling the beam. Therefore, in order for the HXeI molecule to be oriented along the static field, it has to be formed in its ground rotational state, leaving the $J = 1$ state empty. That this is indeed the case is ensured by the cluster environment. For this purpose calculations were carried out for HXeI molecules surrounded by Xe atoms [8]. The relevant processes, the bending vibration and the orientational tilting (libration) mode, turned out to be quite stiff with very small zero point amplitudes in the range of 10° and 2°, respectively. Thus excited rotational modes can be expected to be only marginally populated.

During the process of the HX molecule dissociation and the HXeX molecule creation and orientation, energy is released, which results in sequential evaporation of the cluster. This was demonstrated for HCl [52] and HF [50] in Ar_n clusters. Thus it is plausible to assume that most of the cluster evaporates so that we have to deal with a free HXeI molecule or one with just a few Xe atoms attached to it. The geometry of the smallest ones have been calculated and will be used in the discussion of some experimental results later.

After the HXeX molecule is formed and oriented, it is photodissociated with the laser pulse of 243 nm. Successively the fragment H atoms are ionized by the (2 + 1) REMPI process within the same laser pulse and detected with the WMTOF spectrometer. Since the HRgX is oriented prior to the dissociation with the H atom pointing towards the detector, the resulting arrival times of the nascent protons are shorter than the corresponding times of the zero kinetic energy fragments. Consequently, the measured time-of-flight (TOF) spectra are asymmetric with respect to the zero kinetic energy fragment peak with more intensity on the shorter arrival time side. If the laser light, which aligns the molecule, is polarized at 90° to the detector axis, the linear molecule

cannot be oriented by the extraction field and the TOF spectrum asymmetry disappears. However, as will be shown later, some special molecules of asymmetric top shape can be oriented with the 90° polarization. Therefore, in these special cases, the spectrum asymmetry can still be preserved even at the 90° laser polarization.

5. Results

5.1. *Results for HXeI*

The first xenon hydride compound observed in the gas phase was the HXeI molecule [7]. Figure 9 represents the TOF spectrum of H fragment from photolysis of HI molecule on Xe_n clusters of the mean size $\langle n \rangle = 830$. This spectrum was obtained with the laser field polarization of 0° with respect to the detector axis. For smaller cluster sizes similar spectra were also obtained beginning with the mean cluster size $\langle n \rangle = 110$.

The remarkable feature of this spectrum is its strong asymmetry in intensity. As outlined above, in our experimental arrangement the photolysis of a molecule randomly oriented with respect to the direction to the detector has to result in a TOF spectrum nearly symmetric with respect to the position of the zero kinetic energy fragments. The solid line in figure 9 indicates the symmetric part of the spectrum. It should be noted that the symmetric part was constructed so that the fast- and slow-fragment parts of the TOF spectrum give identical kinetic energy distributions after transformation from a time to energy scale. Thus the slight asymmetry in the TOF spectrum indicated by the line is a manifestation of the fact that the atoms starting in the opposite directions after the photolysis see different electric fields on their way to the detector.

The shaded area in figure 9 corresponds to the pronounced asymmetric part of the spectrum. This is an unambiguous indication for a dissociation of an oriented molecule with H atom pointing in the direction towards the detector. It has been shown in a series of experiments that the dissociation of the HI molecule itself on/in rare gas clusters always resulted in a symmetric TOF spectrum [2, 4, 6, 46]. Clearly the HXeI molecule is the number one candidate for generating the asymmetric part of the spectrum.

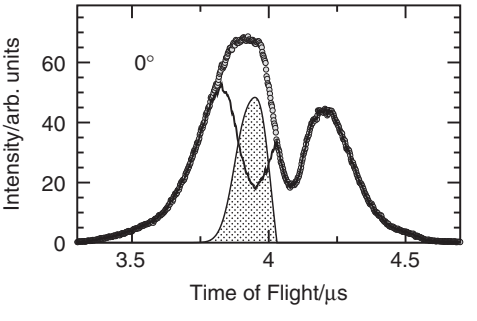

Figure 9. Measured H atom TOF spectrum from the photolysis of HI molecules on Xe_n clusters of the mean size $\langle n \rangle = 830$. The HI molecule was dissociated with 0° polarization laser light at 243 nm. The solid line shows the fit of the symmetric part of the spectrum, the shaded area corresponds to the asymmetric part.

First, this molecule can be generated in our experiment by HI photolysis on Xe_n clusters by the mechanism outlined above, and secondly, its very large dipole moment and polarizability anisotropy allows us to orient this molecule in the combination of the laser field with the weak electric extraction field, as discussed in more detail above. In addition, the long laser pulse duration of $\tau = 5\,\text{ns}$, which corresponds to $\tau/(\hbar/B) \approx 26$, ensures adiabaticity.

In more recent experiments [8] the TOF spectra of H fragments after photolysis of HI molecules on Xe_n clusters were measured with a higher resolution given by a longer drift region of the WMTOF (from 169.8 mm to 320.3 mm). The experiments were carried out in an extended cluster size range from $\langle n \rangle = 107$ to 2017. Figure 10 shows two examples of the TOF spectra for two different mean cluster sizes $\langle n \rangle = 2017$ (top) and 668 (bottom). The spectra were again analysed and split into the symmetric (line) and asymmetric (shaded area) parts. The fact that the asymmetry of these spectra was weaker than for the previous ones could be traced back to the lower nominal intensity of the laser, which reduced the alignment and subsequently the orientation the HXeI molecule.

Figure 11 shows the kinetic energy distribution of the H fragments obtained by the transformation of the symmetric part of the TOF spectra for the two mean cluster sizes $\langle n \rangle = 2017$ and 668 from figure 10. These distributions exhibited the typical pattern for the dissociation of the HI molecule itself in Xe_n clusters. The black arrows at $\approx$2.0 eV and $\approx$1.0 eV mark the energies of the H atoms corresponding to the unperturbed direct cage exit after photolysis, leaving the I atom in the ground and excited spin–orbit states, respectively. The maximum for the direct cage exit after dissociation into the excited I* state agrees well with the position at 1 eV, while the dissociation into the ground state leads to the peak shifted by the energy transfer with the cage to somewhat lower energies. The maximum at zero kinetic

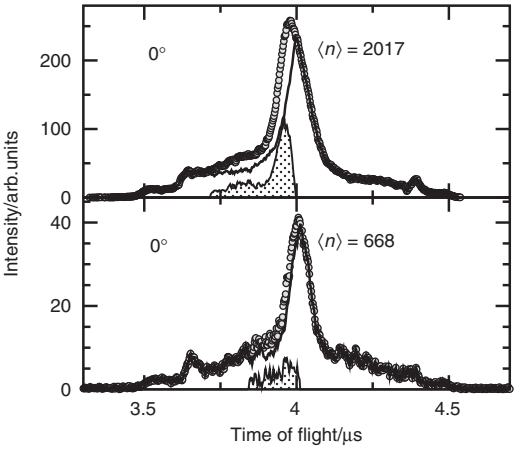

Figure 10. Measured H atom TOF spectra from photolysis of HI molecules on Xe_n clusters of the mean sizes $\langle n \rangle = 2017$ (top) and 668 (bottom). The HI molecules were dissociated with 0° polarization laser light at 243 nm. Solid lines show the fit of the symmetric parts of the spectra, shaded areas correspond to the asymmetric parts.

energy corresponds to the H fragments completely slowed down by the interaction with the surrounding Xe atoms of the cluster. It should be mentioned that photolysis of HI on Kr_n and HBr on Xe_n yielded similar results while for the lighter Ne_n and Ar_n the zero kinetic energy peak is more pronounced [53]. Another noticeable feature is the structure at around 0.3–0.4 eV, indicated by the dashed arrow, attributed to the photodissociation of another species of the HXeX type, namely HXeH molecule, which will be discussed below. However, the focus here is on the asymmetric part which is due to the HXeI molecule.

An additional experimental test was carried out to verify that the asymmetric part of the signal in the TOF spectra originates from the oriented molecules. The idea of the experimental arrangement is schematically sketched in figure 12. On the left hand side, the typical experimental arrangement is shown, with the static electric field E_s pointing towards the detector where the ionized fragments get extracted. In the other arrangement, shown at the right hand side, the orientation of the electric field was kept opposite to the previous experiment during the laser pulse. This resulted in the opposite orientation of the HXeI molecule, i.e. with the H atom pointing away from the detector. Thus the H fragment after the HXeI photolysis started in the direction away from the detector. Approximately 50 ns later, the direction of the E_s field was reversed to accelerate the photolysis fragments back into the detector. Thus the symmetric part of the TOF spectrum remained unchanged but the asymmetry shifted over to the slow fragment region. The results of the measurements with the reversed extraction field is illustrated in figure 13 for the mean cluster size $\langle n \rangle = 983$. The result is a clear indication that the asymmetry is indeed caused by the orientation of the molecules and not by a secondary mechanism which removes one direction of the aligned molecules.

The KED of the H fragments obtained by the transformation of the asymmetric part of the TOF spectra is shown in figure 14. The energy axis was converted

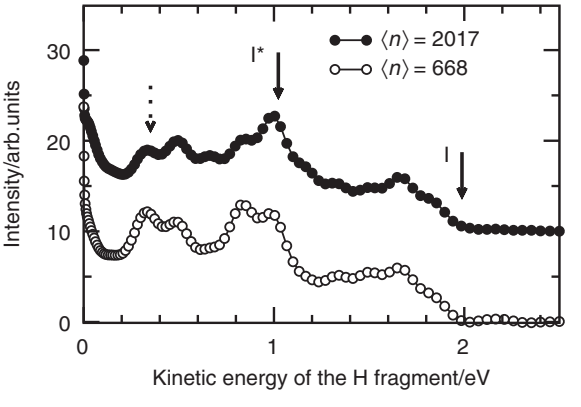

Figure 11. Kinetic energy distributions of the H atoms from HI molecule dissociation on Xe_n clusters $\langle n \rangle = 2017$ (closed) and 668 (open symbols), corresponding to the TOF spectra from figure 10. Solid arrows indicate the nominal cage exit energies related to the two spin-orbit states of I. The structure at the position of the dashed arrow was attributed to the dissociation of the symmetric HXeH molecule.

to cm^{-1} for comparison with spectroscopic studies of these molecules [54]. The distributions exhibited similar structures independent of the mean cluster size and of the extraction field orientation (the bottom curve was obtained from the measurement with the reversed E_s orientation). The distribution covers the energies from 0 to about 3500 cm^{-1} (0.43 eV) which nicely corresponds to the predicted well depth of the HXeI molecule potential. In addition, they exhibit three distinct peaks with approximately equidistant spacing of 1100 cm^{-1}. It should be noted that this quantity agrees with the wavenumber of the Xe–H stretch vibration of 1139 cm^{-1} obtained from the infrared spectroscopy of HXeI molecules in the matrices [54]. A more detailed discussion of how the KED of the H fragment reflects the vibrational structure of the dissociating HXeX molecule is given in the next section, with the explanation of the HXeCl spectra based on the potential energy surfaces available for the HXeCl system.

It is interesting to note that in the case of HI molecule dissociating on the Xe cluster also the perpendicular arrangement of the laser and the extraction field seemed to produce an orientation of a molecule with respect to the detector axis, expressed by the small asymmetry of the TOF spectrum in figure 15. This seemingly contradictory result can be explained by the generation of yet another interesting species, the

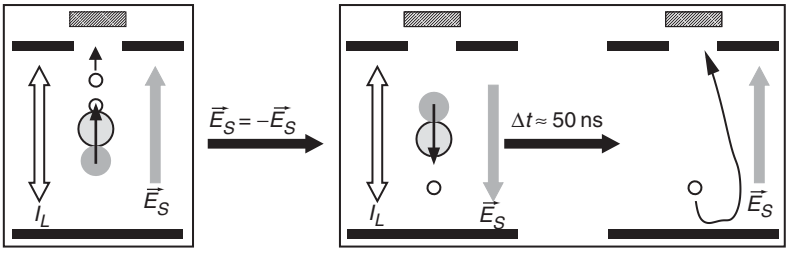

Figure 12. Schematic experimental arrangement for the test of the HXeI molecule orientation. (a) Typical arrangement with the laser polarization parallel to the WMTOF axis and the electrostatic extraction field E_s pointing towards the detector; (b) E_s inverted orientation. 50 ns after the laser pulse, the direction of the E_s field was reversed back to accelerate the ionized photolysis fragments into the detector.

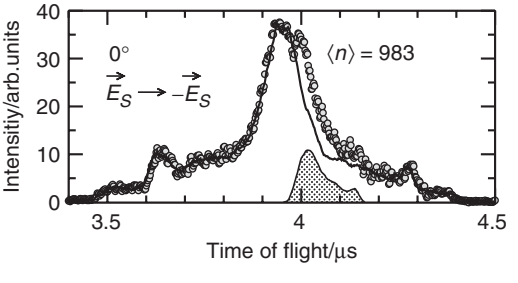

Figure 13. TOF spectra from photolysis of HI molecules on Xe_{983} clusters measured with the inverted electrostatic field arrangement outlined in figure 12. The HI molecules were dissociated with 0° polarization laser light at 243 nm. Solid lines show the fit of the symmetric parts of the spectra, shaded areas correspond to the asymmetric parts, which is now shifted to the opposite side from the central peak with respect to the spectra in figure 10.

HXeI–Xe molecule. During the formation process of the HXeI molecule in photolysis of HI on Xe_n, the cluster begins to evaporate. The final completely oriented state is reached for the bare molecule. However, complexes with one or several Xe atoms attached can be also formed. These complexes tend to have a nearly spherical structure with very low rotational constants, with the exception of HXeI–Xe, which is an asymmetric top molecule schematically drawn in figure 16. The polarizability of this molecule in the direction perpendicular to the direction of the HXeI moiety axis was estimated to have the largest value. This in turn would lead to the alignment of this molecule in the strong laser field with 90° polarization such that the HXeI moiety would be parallel to the detector axis [55]. The additional interaction with the extraction

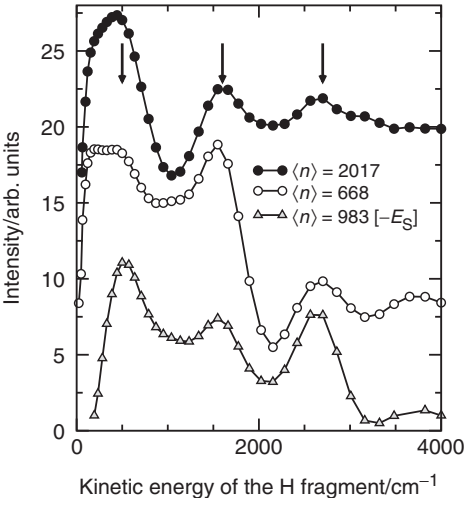

Figure 14. Kinetic energy distributions of the H atoms from HI molecule dissociation on Xe_n clusters. The KEDs are obtained by the transformation of the asymmetric part of the TOF spectra shown in figures 10 and 13. The bottom curve (triangles) is derived from the measurement with the reversed E_S orientation. The energy axis is converted to cm^{-1} for comparison with spectroscopic studies.

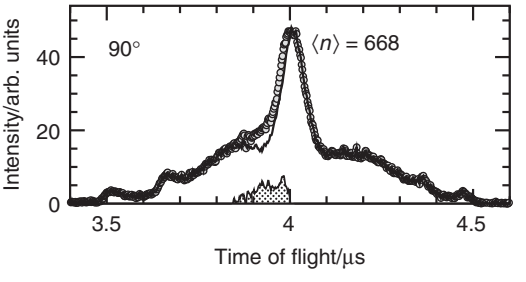

Figure 15. Measured H atom TOF spectrum from photolysis of HI molecule on Xe_{668} clusters with 90° polarization laser light at 243 nm. Solid line shows the fit of the symmetric part of the spectrum, shaded area corresponds to the asymmetric part.

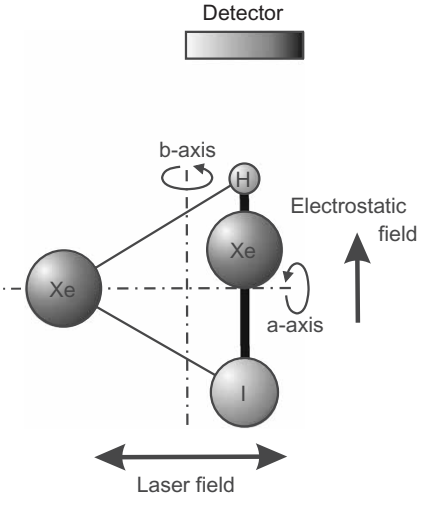

Figure 16. A schematic picture of the asymmetric top molecule, HXeI–Xe. The strong polarizability along the *a*-axis leads to the alignment in the strong laser field with 90° polarization such that the HXeI moiety would be parallel to the detector axis. The additional interaction with the extraction electric field turns this alignment into the orientation, such that the H atom of the HXeI moiety points to the detector.

electric field would then turn this alignment into the orientation, such that the H atom of the HXeI moiety would point to the detector. Thus the observation of the TOF spectrum asymmetry at 90° polarization is an indication for the generation and orientation of the asymmetric top molecule HXeI–Xe.

5.2. *Results for HXeCl*

Figure 17 shows the TOF spectra of H fragments from HCl molecules dissociated on the Xe_n clusters of the mean cluster size $\langle n \rangle = 1020$. In this experiment two lasers were used, as outlined in the experimental section: 193 nm for dissociation of HCl molecules, and 243 nm to ionize the H atom fragments. The laser polarization of 0° and 90° indicated on the top and bottom panel, respectively, corresponds to the dissociation laser field. The ionization laser was 0° polarized in both cases. The top TOF spectrum measured with the 0° polarization of the photodissociation laser exhibited a clear asymmetry. The solid line shows a simulation fit of the symmetric part of the spectrum. The difference between the asymmetric experimental spectrum (circles) and the symmetric simulated spectrum (solid line) exhibited again, as in the case of HI dissociation on Xe_n, a maximum on the side of the faster than zero kinetic energy fragments. This spectrum (shaded area) corresponds to the H atoms resulting from the dissociation of the oriented HXeCl molecule. The spectrum asymmetry is not preserved, if the dissociation laser polarization is turned to 90°. This is consistent with the HXeCl molecule not being oriented any more in the direction of the detector axis. However, it is worth noting that the situation is complicated by the presence of the two laser fields. The ionization 243 nm laser light is polarized at 0° as before.

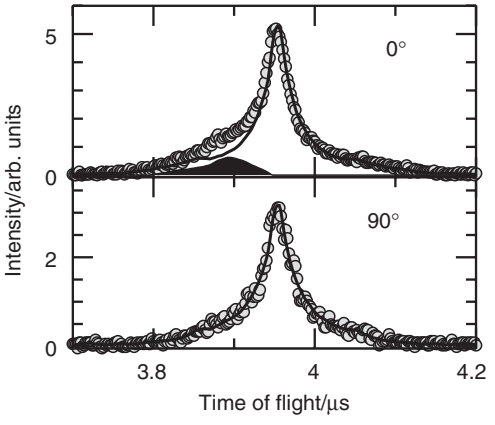

Figure 17. Measured TOF spectra of H atoms from HCl molecule dissociation on Xe_{1020} clusters. The spectrum obtained with the 0° laser polarization (193 nm) exhibits an asymmetry attributed to the dissociation of the oriented HXeCl molecule (upper panel), while the spectrum corresponding to the 90° polarization is symmetric (lower panel).

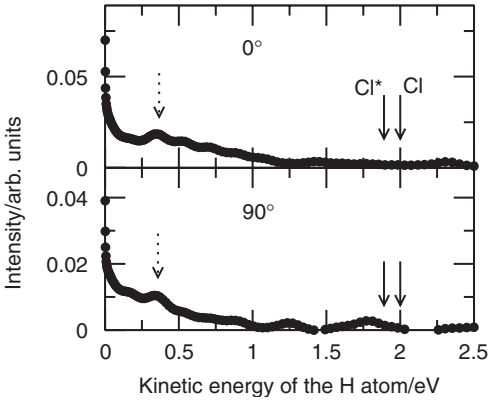

Figure 18. KED of H fragments from the dissociation of the HCl molecule on Xe_n clusters obtained from the symmetric part of the TOF spectrum in figure 17.

Yet, in this case, this laser field alone does not seem to be sufficient to align the molecule in the detector direction.

The KED obtained by fitting the symmetric part of the TOF spectra in figure 17 is represented in figure 18. These distributions show almost no evidence for the direct cage exit process of the H atom after the dissociation, which would appear around 2 eV. The intensity peaks at 0 eV, corresponding to the caging, and extends to about 1 eV corresponding to the delayed cage exit with some energy transfer to the cage. A noticeable feature is the peak at approximately 0.3 eV, which has been attributed to the dissociation of another Xe molecule, HXeH, discussed in the next section.

The asymmetric part of figure 17, which corresponds to the dissociation of the HXeCl molecule, was transformed into the KED shown in figure 19. The distribution extends

to approximately 700 cm^{-1} (0.8 eV), which is consistent with the estimated range of the bonding energy of the HXeCl molecule of about 0.9 eV. There is a superimposed structure on the spectrum significant with respect to the experimental errors of 10–30%, similar to the case of HXeI molecule discussed above. This structure revealed some details of the dissociation mechanism, and can be discussed in terms of the potential energy surfaces. Since there has been no theoretical evidence for a repulsive state crossing directly the ground state of HXeCl [17], the molecule has been proposed to transfer to an electronically excited state crossed by a repulsive state decaying into $H + XeCl^*$, as indicated by the calculated potential energy curves in figure 20. This picture can be used to interpret the observed structure in figure 19 in terms of the Xe–H stretch vibrations of the HXeCl molecule.

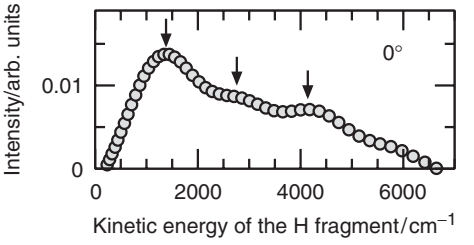

Figure 19. KED of H fragments from the dissociation of the oriented HXeCl molecule obtained from the asymmetric part of the upper TOF spectrum in figure 17.

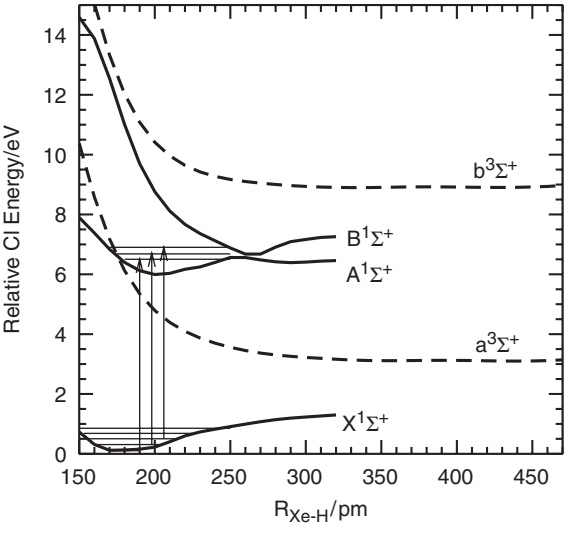

Figure 20. Calculated potential energy surfaces of HXeCl molecule along the H–Xe coordinate [17]. The arrows indicate the transitions between the vibrational states $v = 0,1,2$ of the ground electronic states and the corresponding vibrations of the B-state close to the A–B state crossing. The arrows have constant length corresponding to the 193 nm (6.4 eV).

It has to be kept in mind that the molecule is excited at a constant wavelength 193 nm which corresponds to 6.4 eV energy. Transitions from a manifold of three lowest vibrational states in the electronic ground state into a manifold of vibrational states in the electronically excited B-state were considered. If these transitions land energetically close to the crossing point of the B-state with the repulsive A-state, as indicated by the arrows in figure 20, the kinetic energy of the fragments would reflect the vibrational spacing of the molecule in the ground X-state. The difference between the peaks in figure 19 of approximately $1380\,\mathrm{cm}^{-1}$ is in reasonable agreement with the experimental and calculated frequency of the $v=0\rightarrow 1$ transition of $1648\,\mathrm{cm}^{-1}$ [11, 54]. The somewhat lower frequency in our experiment points to a production of higher excited vibrational states in the X-state which, due to the anharmonicity, have a smaller vibrational spacing. Electronic excitation from these states can be achieved by the larger wavelength laser at 243 nm (5.1 eV). Explanation of the generation of the vibrationally excited HXeCl molecules follows directly from the creation mechanism: after the HCl photodissociation the H atom is reflected from the next Xe layer and trapped by the Xe–Cl fragment. Ionic bonds are formed and stabilization of the highly vibrationally excited species proceeds by interactions with the cluster Xe atoms, but probably not all the excess energy is released in this process.

It is worth mentioning that, as opposed to the HI case, the TOF spectrum of the HCl molecule dissociated on the Xe_n cluster with the 90° polarized laser did not exhibit any asymmetry (see figure 17). An explanation for this result can be the somewhat different experimental arrangement in the experiment with HCl with respect to the one with HI. Namely the combination of the two laser fields employed in the HCl experiment in perpendicular arrangement resembled an elliptical polarization, which breaks the coupling of the pulsed laser field to the static field.

5.3. *Other molecules*

We tried to extend the measurements also to other systems. In the case of the photodissociation of HBr on Xe_n clusters we did not observe any asymmetry in the time-of-flight spectrum [56]. The same was true for HI and HBr on Kr_n clusters [53] and HCl on Kr_n clusters [56]. To verify this behaviour, we have calculated the $\Delta\omega$ and the ω parameter which determine the orientation. The results for selected systems are also presented in table 2 together with the data of the two systems HXeI and HXeCl which were successfully detected by their orientation. The value of $\Delta\alpha$ was calculated from the polarizability α of the constituents using a relation between $\Delta\alpha$ and α derived from similar ionically bound systems. A consistency check was carried out by considering the calculated polarizabilities of the isoelectronic, ionically bound alkali halide molecules [57]. We note that these values can only be considered as estimates, since there are obvious uncertainties in $\Delta\alpha$ and in the effective laser intensities. As expected, the values for $\Delta\omega$ decrease with decreasing masses of the molecules. For HXeCl this is partly compensated for by the increasing laser intensity originating from the second laser in the interaction region. To get information about the degree of orientation, the direction cosine $\langle\cos\theta_s\rangle$ was calculated by solving the Schrödinger equation using the procedure described in detail in [58] and the results presented in figure 3. The values for the direction cosine $\langle\cos\theta_s\rangle$ and the corresponding angular amplitude

θ_s clearly indicate that for the latter parameters a value of $\theta_s \leq \pm 30^\circ$ or $\langle \cos \theta_s \rangle \geq 0.86$ is necessary to detect the asymmetry in our experimental arrangement. For HXeBr the value of $\theta_s \leq \pm 54.3^\circ$ is apparently too large to see a signature of oriented HXeBr molecules. Similar considerations hold for the HKrCl where the same relation holds. This does, of course, not mean that these molecules do not exist in the gas phase. But they cannot be detected in our experimental arrangement.

Another very interesting molecule of the new type is HXeH. Because of its symmetry, it is not possible to orient this molecule. It was, however, observed in the KED obtained by transformation of the symmetric part of the TOF spectrum of emitted H atoms. The bonding energy of these species is estimated to vary between 0.32 and 0.48 eV [13]. This coincides with the small peak at around 0.35 eV indicated already above in figures 11 and 18. These spectra are summarized in figure 21. In this figure the spectrum with HCl molecule was obtained with the unpolarized 193 nm light, i.e. with higher laser field intensity, which results in a more pronounced peak at 0.35 eV than in in figure 18. Also the measurement with HBr molecules on Xe_n clusters is included in this figure. Although no indication for generation of an oriented HXeBr

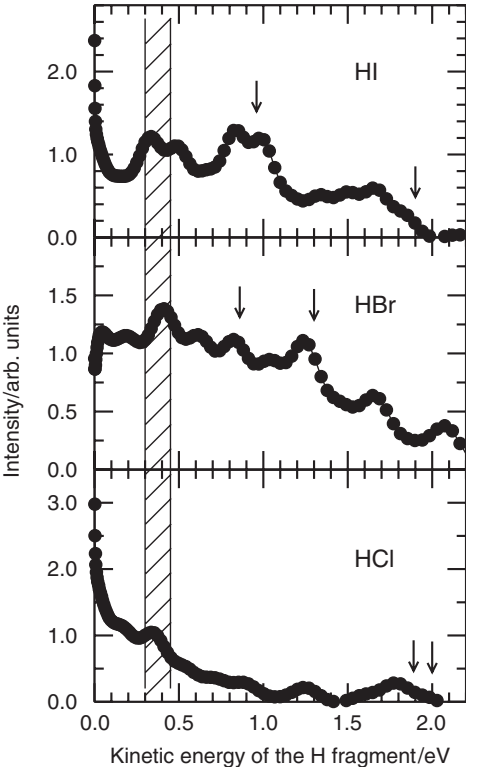

Figure 21. Comparison of the KEDs from the dissociation of HI, HBr and HCl (from top to bottom) molecules on Xe clusters. The peaks at approximately 0.35 eV (in the hatched area) correspond to the photodissociation of the symmetric HXeH molecules. The arrows indicate the spin–orbit states of the halogen atoms.

molecule was found in these experiments (presumably this molecule was generated but not oriented under our experimental conditions), the peak at 0.35 eV suggested the production of the HXeH molecule from HBr photolysis. Although other spectral features, e.g. the cage exit peaks, were quite different in the three KEDs, the pronounced peak around 0.35 eV (hatched area) was present in all of them, which suggested a common origin of this spectral feature: the HXeH molecule. It can be generated by the photolysis of the hydrogen halides molecules on Xe_n clusters. Indeed, the necessary condition for generating the HXeH molecule is the dissociation of more than one hydrogen-containing molecule on the cluster. However, in the pick-up process of the larger clusters considered here more than one HX molecule can be embedded. Besides, pick-up of hydrocarbon molecules from the background pressure cannot be excluded. These hydrocarbons can be also dissociated at our wavelengths. The HXeH molecules can be also dissociated at the wavelength of our two lasers, which operate at 243 nm and 193 nm. Studies in matrices show that HXeH can be easily dissociated in a wavelength range between 180 nm and 350 nm [27].

6. Summary and prospects

A new class of molecules of the type HRgX was identified in the gas phase after the photodissociation of hydrogen halide molecules HX in rare gas clusters Rg_n. By accompanying calculations the mechanism of the formation was clarified. The H atom leaves the cage, is reflected from the next shell of rare gas atoms, and recombines with the RgX moiety to form HRgX. The energy release leads to a sequential evaporation of the cluster. Then the HRgX molecule is oriented in a combined strong laser field and a weak static electric field in such a way that the H atom points into the direction of the detector. After the photolysis of this oriented molecule, the asymmetric distribution of H atoms is observed. Up to now only two molecules were detected in this way, HXeI and HXeCl. There is a trade-off between the stability of these molecules and the ability to orient them. The stability increases with increasing electron affinity and smaller sizes, thus decreasing mass of the halogen atom. The orientation clearly favours large masses, since the anisotropy of the polarizability increases with volume. Therefore, the first molecule detected in this way was the heavy HXeI [8]. In this case only one laser at 243 nm was used for the photodissociation of HI and HXeI and the detection of the H atoms. Here the static electric field and the laser field were parallel to each other. For HXeCl two laser pulses were used, one at 193 nm for the photolysis of HCl and the other at 243 nm for the dissociation of HXeCl and the detection of the H atoms. The asymmetric signal was present with both lasers and the electric field in the same direction. The effect disappeared if one of the lasers is polarized perpendicular to the other laser and the static field. We investigated also HXeBr [56] and the Kr containing systems after the photolysis of HI, HBr [53], and HCl [56]. In none of these cases any HRgX molecules were detected. In the case of HXeBr the laser intensity turned out to be too small (here only one laser was used), while for HKrCl the polarizabilty was not large enough to produce a detectable signal at the detector. Apparently, our experimental arrangement requires a very high

orientation, $\langle\cos\theta_s\rangle \geq 0.8$, to give a detectable signal. The molecules HKrI and HKrBr have not yet been found, neither in experiment nor in calculations. They probably do not exist. What would help in improving the experimental situation, would be a higher laser intensity for the alignment process. This can be relatively easily achieved in our experimental arrangement, if we apply the fundamental of the YAG laser which has an intensity of 700 mJ/pulse instead of the 1.8 mJ/pulse at 243 nm. Then we would end up with intensities in the range of 10^{13} W/cm^2 which would automatically lead to much higher $\Delta\omega$ and thus higher $\langle\cos\theta_s\rangle$ values.

Higher laser intensities (up to 260 mJ/pulse) were also applied in the only other measurement available for orienting molecules by applying the technique of combined strong laser and weak electrostatic fields by the group of Sakai [59, 60]. The key parameters for the investigated OCS molecules, $\Delta\omega = 200$ and $\omega = 0.022$, are close to those obtained for HXeI. The smaller dipole moment is compensated by a higher extraction field. In spite of these favourable numbers, which would lead to a direction cosine $\langle\cos\theta_s\rangle$ close to 0.96 for the rotational ground state, the overall averaged direction cosine estimated for these experiments is $\langle\cos\theta_s\rangle = 0.43$. The reason is that for the estimated rotational temperature of 1 K higher rotational states contribute to the signal with the reversed orientation. Nevertheless the orientation was detected by photodissociation, since, in contrast to the present experiment, the signal is free of contribution from other competing processes.

Aside from the unambiguous detection of the HRgX molecules by their orientation, also the measured kinetic energy can be used for identification. This was applied to the molecule HXeH which cannot be oriented. Its existence was proved by a peak in the kinetic energy distribution of the H atoms of all three measured system HI–, HBr–, and HCl–Xe$_n$ at the correct energy loss predicted by calculations. In addition, the dissociation mechanism of HXeCl was clarified by a comparison with available calculations of the potential surfaces. It proceeds via a curve crossing in the electronically excited state and the structure in the measured kinetic energy distribution reflects the vibrational states in the Xe–H potential curves.

Discussing the extension of the present work, it should be possible to detect less polarizable and more stable HRgX molecules by increasing the laser intensity. Very promising species are those which contain –OH, –SH, and –CN fragments [21, 27, 61]. A very intriguing result is the detection of HKrCCH [28] and HXeCCH, HXeCC, and HXeCCXeH [24] in cold matrices. These results open up a new organo-rare gas chemistry. The preparation of such species in the gas phase should be possible starting with the photolysis of acetylene C_2H_2. An interesting issue is also the formation of complexes of HRgX molecules with other molecules. A nice example is the interaction of HXeOH with water molecules which exhibits stabilizing and destabilizing effects [30].

Acknowledgments

We dedicate this article to Roger Miller who left us so early. The orientation of molecules in pendular states and the high-resolution spectroscopy of these molecules was one of his central fields of research. His advice in the early stages of this experiment

was extremely valuable to us. We thank Bretislav Friedrich for introducing us to the world of oriented molecules and for his help in calculating the degree of orientation. We are grateful to Benny Gerber and Zolt Bihary for useful calculations on the formation and the rotation of the hydride molecules. Last but not least we thank the two doctoral students Reinhard Baumfalk and N. Hendrik Nahler who measured and evaluated most of the data presented here. We acknowledge useful discussions with Mika Pettersson and Leonid Khriachtchev on the behaviour of the new rare gas hydride molecules. This work was supported by the Deutsche Forschungsgemeinschaft in SFB 357. MF acknowledges the Alexander von Humboldt fellowship.

References

[1] U. Buck, J. Phys. Chem. A **106**, 10049 (2002).
[2] P. Slavíček, P. Žďánská, P. Jungwirth, R. Baumfalk, and U. Buck, J. Phys. Chem. **104**, 7793 (2000).
[3] N. H. Nahler, M. Fárník, U. Buck, H. Vach, and R. B. Gerber, J. Chem. Phys. **121**, 1293 (2004).
[4] P. Slavíčcek, P. Jungwirth, M. Lewerenz, N. H. Nahler, M. Fárník, and U. Buck, J. Chem. Phys. **120**, 4498 (2004).
[5] M. Fárník, N. H. Nahler, U. Buck, P. Slavíček, and P. Jungwirth, Chem. Phys. **315**, 161 (2005).
[6] P. Slavíček, P. Jungwirth, M. Lewerenz, N. H. Nahler, M. Fárník, and U. Buck, J. Phys. Chem. A **107**, 7743 (2003).
[7] R. Baumfalk, N. H. Nahler, and U. Buck, J. Phys. Chem. **114**, 4755 (2001).
[8] N. H. Nahler, U. Buck, Z. Bihary, R. B. Gerber, and B. Friedrich, J. Chem. Phys. **119**, 224 (2003).
[9] B. Friedrich and D. Herschbach, J. Phys. Chem. A **103**, 10280 (1999).
[10] B. Friedrich and D. Herschbach, J. Chem. Phys. **111**, 6157 (1999).
[11] M. Pettersson, J. Lundell, and M. Räsänen, J. Chem. Phys. **102**, 6423 (1995).
[12] M. Pettersson, L. Khriachtchev, J. Lundell, and M. Räsänen, in *Inorganic Chemistry in Focus II*, edited by G. Meyer, D. Naumann, and L. Wesemann (Wiley-VCH, Weinheim, 2005), p. 15.
[13] M. Pettersson, J. Lundell, and M. Räsänen, Eur. J. Inorg. Chem. **5**, 729 (1999).
[14] J. Lundell, L. Khriachtchev, M. Pettersson, and M. Räsänen, Low. Temp. Phys. **26**, 680 (2000).
[15] R. B. Gerber, Ann. Rev. Phys. Chem. **55**, 55 (2004).
[16] I. Last and T. F. George, J. Chem. Phys. **89**, 3071 (1988).
[17] M. Johansson, M. Hotokka, M. Pettersson, and M. Räsänen, Chem. Phys. **244**, 25 (1999).
[18] J. Lundell, M. Pettersson, L. Khriachtchev, M. Räsänen, G. M. Chaban, and R. B. Gerber, Chem. Phys. Lett. **322**, 389 (2000).
[19] J. Panek, Z. Latajka, and J. Lundell, Phys. Chem. Chem. Phys. **4**, 2504 (2002).
[20] M. Pettersson, J. Nieminen, L. Khriachtchev, and M. Räsänen, J. Chem. Phys. **107**, 8423 (1997).
[21] M. Pettersson, J. Lundell, L. Khriachtchev, and M. Räsänen, J. Chem. Phys. **109**, 618 (1998).
[22] G. M. Chaban, J. Lundell, and R. B. Gerber, Chem. Phys. Lett. **364**, 628 (2002).
[23] L. Khriachtchev, M. Pettterson, J. Lundell, and M. Räsänen, J. Chem. Phys. **114**, 7727 (2001).
[24] L. Khriachtchev, H. Tanskanen, J. Lundell, M. Pettersson, H. Kiljunen, and M. Räsänen, J. Am. Chem. Soc. **125**, 4696 (2002).
[25] A. Cohen, M. Y. Niv, and R. B. Gerber, Faraday Discuss. **118**, 269 (2001).
[26] M. Pettersson, L. Khriachtchev, L. Lundell, and S. J. and, J. Phys. Chem. A **104**, 3579 (2000).
[27] L. Khriachtchev, H. Tanskanen, M. Pettersson, M. Räsänen, J. Ahokas, H. Kunttu, and V. Feldman, J. Chem. Phys. **116**, 5649 (2002).
[28] L. Khriachtchev, H. Tanskanen, A. Cohen, R. B. Gerber, J. Lundell, M. Pettersson, H. Kiljunen, and M. Räsänen, J. Am. Chem. Soc. **125**, 6876 (2003).
[29] A. Lignell, L. Khriachtchev, M. Pettersson, and M. Räsänen, J. Chem. Phys. **117**, 961 (2002).
[30] A. V. Nemukhin, B. L. Grigorenko, L. Khriachtchev, H. Tanskanen, M. Pettersson, and M. Räsänen, J. Am. Chem. Soc. **124**, 10706 (2002).
[31] J. Reuss, in *Atomic and Molecular Beam Methods*, edited by G. Scoles (Oxford, New York, 1988), p. 276.
[32] J. M. Rost, J. C. Griffin, B. Friedrich, and D. R. Herschbach, Phys. Rev. Lett. **68**, 1299 (1992).
[33] H. J. Loesch and A. Remscheid, J. Phys. Chem. **95**, 8194 (1991).

[34] H. J. Loesch, Ann. Rev. Phys. Chem. **46**, 555 (1995).
[35] B. Friedrich and D. Herschbach, Nature **353**, 412 (1991).
[36] P. Block, E. Bohac, and R. E. Miller, Phys. Rev. Lett. **68**, 1303 (1992).
[37] J. J. Larsen, H. Sakai, C. P. Safvan, I. Wendt-Larsen, and H. Stapelfeldt, J. Chem. Phys. **111**, 7774 (1999).
[38] J. J. Larsen, K. Hald, N. Bjerre, H. Stapelfeldt, and T. Seidemann, Phys. Rev. Lett. **85**, 2470 (2000).
[39] J. Oritigoso, M. Rodriguez, M. Gupta, and B. Friedrich, J. Phys. Chem. **110**, 3870 (1999).
[40] M. N. R. Ashfold, I. R. Lambert, D. H. Mordaunt, G. P. Morley, and C. M. Western, J. Phys. Chem. **96**, 2938 (1992).
[41] C. Maul and K.-H. Gericke, J. Phys. Chem. A **104**, 2531 (2000).
[42] D. W. Chandler and P. L. Houston, J. Chem. Phys. **87**, 1445 (1987).
[43] J. A. Syage, Chem. Phys. **207**, 411 (1996).
[44] L. Schnieder, W. Meier, K. H. Welge, M. N. R. Ashfold, and C. M. Western, J. Chem. Phys. **92**, 7027 (1990).
[45] H. J. Hwang and M. El-Sayed, Chem. Phys. Lett. **170**, 161 (1990).
[46] R. Baumfalk, N. H. Nahler, U. Buck, M. Y. Niv, and R. B. Gerber, J. Chem. Phys. **113**, 329 (2000).
[47] R. Baumfalk, U. Buck, C. Frischkorn, N. H. Nahler, and L. Hüwel, J. Chem. Phys. **111**, 2595 (1999).
[48] R. J. LeRoy, G. T. Kraemer, and S. Manzhos, J. Chem. Phys. **117**, 9353 (2002).
[49] S. R. Langford, P. M. Regan, A. J. Orr-Ewing, and M. N. R. Ashfold, Chem. Phys. **231**, 245 (1998).
[50] T. Schröder, R. Schinke, S. Liu, Z. Bačić, and J. W. Moskowitz, J. Chem. Phys. **103**, 9228 (1995).
[51] R. Baumfalk, U. Buck, C. Frischkorn, S. R. Gandhi, and C. Lauenstein, Ber. Bunsenges. Phys. Chem. **101**, 606 (1997).
[52] M. Y. Niv, A. I. Krylov, R. B. Gerber, and U. Buck, J. Chem. Phys. **110**, 11047 (1999).
[53] R. Baumfalk, N. H. Nahler, and U. Buck, Faraday Disscus. **118**, 247 (2001).
[54] J. Lundell, M. Pettersson, L. Khriachtchev, M. Räsänen, G. M. Chaban, and R. B. Gerber, Chem. Phys. Lett. **322**, 389 (2000).
[55] J. J. Larson, K. Hald, N. Bjerre, and H. Stapelfeldt, Phys. Rev. Lett. **85**, 2470 (2000).
[56] N. H. Nahler, M. Fárník, and U. Buck, Chem. Phys. **301**, 173 (2004).
[57] S. L. Davies, J. Chem. Phys. **88**, 1080 (1988).
[58] B. Friedrich, N. H. Nahler, and U. Buck, J. Mod. Opt. **50**, 2677 (2003).
[59] S. Minemoto, H. Nanjo, H. Tanji, T. Suzuki, and H. Sakai, J. Chem. Phys. **118**, 4052 (2003).
[60] H. Sakai, S. Minemoto, H. Nanjo, H. Tanji, and T. Suzuki, Phys. Rev. Lett. **90**, 083001 (2003).
[61] J. Ahokas, H. Kunttu, L. Khriachtchev, M. Pettersson, and M. Räsänen, J. Phys. Chem. A **106**, 7743 (2002).
[62] G. Maroulis, Chem. Phys. Lett. **318**, 181 (2000).